Journal of Alloys and Compounds 509 (2011) 7356–7360

Contents lists available at ScienceDirect

Journal of Alloys and Compounds

journal homepage: www.elsevier.com/locate/jallcom

Anelastic relaxation caused by interstitial atoms in β-type sintered Ti–Nb alloys

Z.C. Zhou[a,*], J.Y. Xiong[b], S.Y. Gu[a], D.K. Yang[b], Y.J. Yan[a], J. Du[a]

[a] Suzhou Vocational University, Suzhou, 215104 Jiangsu, China
[b] Institute for Technology Research and Innovation, Deakin University, Victoria 3217, Australia

ARTICLE INFO

Article history:
Received 6 December 2010
Received in revised form 14 April 2011
Accepted 16 April 2011
Available online 23 April 2011

Keywords:
Internal friction
Ti–Nb alloys
Interstitial atoms
Nb content
Heat treatment

ABSTRACT

The internal friction behavior of Ti–Nb alloys is investigated using a dynamic mechanical analysis (DMA) Q800 from TA Instruments in single cantilever mode. Relaxational internal friction peaks are found on the internal friction temperature dependent curves in the sintered alloys. The peak does not appear in the sintered Ti–Nb alloys with low Nb content. The water-quenched Ti-35.4 (wt.%) Nb alloy has much higher the internal friction peak than the as-sintered alloy with identical compositions. Therefore, the peak height depends on heat treatment and Nb content. It is deduced that the peak is linked to the β phase of Ti–Nb alloys and that the peak height is determined by the stability and amount of the β phase. When the stability of the β phase is decreased, the peak height is increased. The increase in the amount of β phase results in the increase of the peak height. The β phase in the quenched Ti-35.4Nb specimen is metastable β phase (β_M), which can be transformed into the stable α and β_S by aging. The β phase in as-sintered specimen is the stable β phase (βS). The modifications in microstructures results in the difference between the two Ti-35.4Nb specimens with different states in their peak heights. The peak height presents a maximum in the vicinity of 35 wt.% Nb for the quenched alloys, resulting from the variation of the stability and amount of β_M with Nb content. In as-sintered alloys, the height of the peak increases monotonously with increasing Nb content due to the increase of the amount of β_S. It has been suggested that the internal friction peak is related to oxygen jumps in lattice and the interactions of oxygen-substitute atoms in β_M for the water-quenched alloys and in β_S phase for the as-sintered alloys.
© 2011 Elsevier B.V. All rights reserved.

1. Introduction

When Ti–Nb alloys were water-quenched from the high temperature β phase that possesses single disorder body-centered cubic (bcc) structure, the formation of the equilibrium low temperature α phase with hexagonal close-packed (hcp) structure and the stable β phase (β_S) is suppressed. The high temperature β phase can be retained by quenching to room temperature, obtaining the so-called metastable β (β_M). By contrast, if the alloys were annealed from high temperature, the stable α and β_S phases would be produced [1].

The presence of interstitial atoms (C, N, O and H) has great effects on the physical, chemical and mechanical properties of most metallic materials, which is also true for elastic and anelastic properties [2]. It has been known that point defects in crystalline solids can generate a time-dependent strain under the application of an external cycle stress due to the reorientation of the point defects. The phenomenon was experimentally investigated in α-Fe with interstitial impurities of carbon or nitrogen by Snoek in 1941 [3]. Recently, Saitoh et al. investigated the influences of substitutional atoms on the Snoek peak of carbon in bcc iron [4–6]. In β-type Ti–Nb alloys, the Snoek relaxation peak is caused by oxygen and/or nitrogen [2,7–11]. However, it is not yet clear which changes of the relaxation correlated to oxygen and/or nitrogen may take place when the microstructures of the sintered Ti–Nb alloys are varied by the compositions and heat treatment. The aim of the present research, therefore, is to make clear the effects of chemical composition and heat treatment on the internal friction peak of the β-type Ti–Nb alloys by studying the internal friction behavior of the Ti–Nb alloys.

2. Experimental procedures

Ti–Nb alloy samples were prepared by powder metallurgy. Commercially available elemental metal powders of Ti (purity 99.8%, particle size 325 mesh) and Nb (purity 99.8%, particles size325 mesh) were used as starting materials. The powder handling was conducted in argon gas atmosphere. Ti and Nb powders with different nominal Nb mass concentrations of 12, 20, 30, 35.4, 41 and 45 were blended using a planetary ball-milling machine (Retsch PM400) at 110 rpm for 2 h. The weight ratio of ball to powder was 2:1. Ti–Nb rectangle samples with a size of $100 \times 10 \times 5\ mm^3$ were prepared by consolidating the metal powder mixture at 1450 bar (atmosphere pressure) and then sintering at 1200 °C for 5 h in a vacuum of 10^{-5}–10^{-6} Torr (CAMCoG-VAC 12). The surface of the sintered Ti–Nb samples were ground using silicon carbide papers to a 1200 grit finish.

* Corresponding author. Tel.: +86 512 66875482.
E-mail address: zhouzhengcun@126.com (Z.C. Zhou).

0925-8388/$ – see front matter © 2011 Elsevier B.V. All rights reserved.
doi:10.1016/j.jallcom.2011.04.090

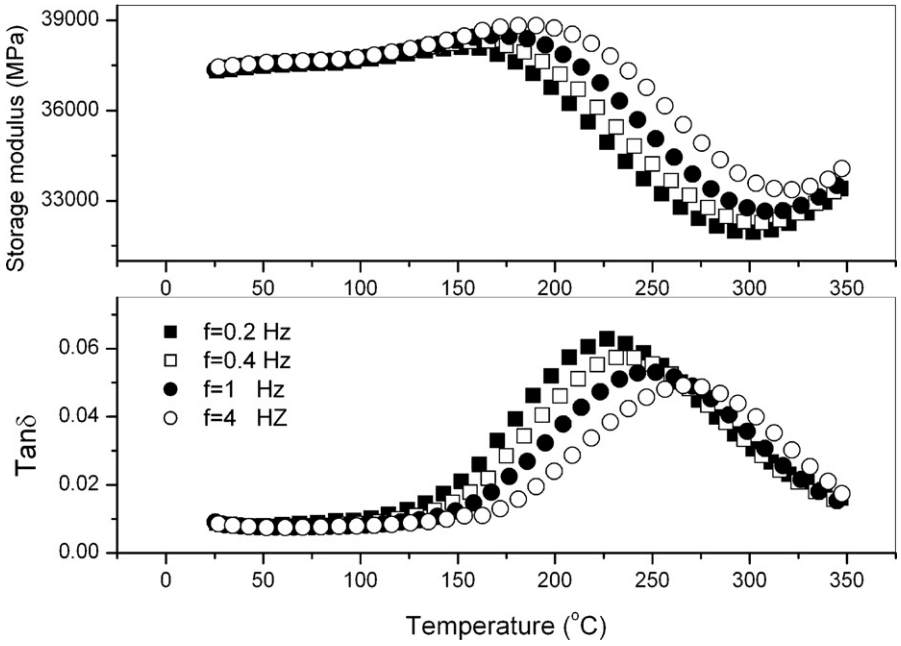

Fig. 1. Tanδ and storage modulus as a function of temperature for the water-quenched Ti-35.4 Nb alloy at different vibration frequencies ($\varepsilon = 3 \times 10^{-4}$).

The specimens for the internal friction measurements ($4.5 \times 1.2 \times 30\,mm^3$) were spark cut from the rectangle sample. They are homogenized at 1000 °C for 1 h, and then quenched into water. The internal friction (Tanδ, δ is loss angle between stress and strain) and storage modulus were measured using a dynamic mechanical analysis (DMA) Q800 from TA Instruments in single cantilever mode ($\varepsilon = (2.4–4.3) \times 10^{-4}$) for the as-sintered and water-quenched (WQ) specimens. Two measurements at $\varepsilon = 3 \times 10^{-4}$ and $\varepsilon = 5.6 \times 10^{-4}$ was also performed for the water-quenched Ti-35.4Nb alloy to investigate the effect of strain amplitude on the internal friction peak. Four frequencies (0.2, 0.4, 1, 4 Hz) were swept when the specimens were heated with a temperature rate of 6 °C/min since sufficient data can be obtained for the above four frequencies at the heating rate. The thermal cycling of the quenched Ti-35.4Nb specimen was performed between room temperature and 350 °C by the in situ heating/cooling of the specimen in the instrument and the data of Tanδ and storage modulus during heating was recorded for 6 times. In addition, X-ray diffraction experiments were also carried out in order to detect the differences in the microstructures of the specimens with different heat treatments for the Ti-35.4Nb alloy.

3. Results and discussion

3.1. The internal friction in the Ti–Nb alloys

Fig. 1 shows the Tanδ and storage modulus of the water-quenched Ti-35.4Nb alloy as a function of temperature during heating at different vibration frequencies. It can be seen that an internal friction peak appears at around 250 °C and the storage modulus declines at the peak position according to Kronig–Kramers relation [2,3]. The peak is shifted to higher temperature when the vibration frequency is increased, indicating that the peak is a thermally activated relaxation process. The peak has not dependence on amplitude and the peak position and height are kept unchanged when amplitude is raised, as shown in Fig. 2, being an evidence of linear anelastic relaxation.

For a thermally activated relaxation process with a single relaxation time, the relaxation time τ follows the Arrhenius law [3]:

$$\tau = \tau_0 \exp\left(\frac{H}{kT}\right) \quad (1)$$

Where τ_0 is the pre-exponential factor and H is the activation energy of the relaxation process. At the peak position, $\omega\tau_p = 1$ is satisfied, where $\omega = 2\pi f$ is the angular frequency and τ_p is the relaxation time at the peak temperature. Relaxation parameters can be calculated from Fig. 1 to be $H_{wq} = 1.67 \pm 0.1$ eV and $\tau_{0wq} = 1.1 \times 10^{-17}$ s for the water-quenched Ti-35.4Nb alloy at the heating rate of 6 °C/min. For the heating rate of 3 °C/min., the activation parameters are $H'_{wq} = 1.66 \pm 0.06$ eV and $\tau'_{0wq} = 1.7 \times 10^{-17}$ s, indicating that the influence of the heating rate on the activation parameters can be neglected. From these activation parameters, the present internal friction peak is similar to those reported in Refs. [7–12]. Oxygen jumps in bcc solution are the main physical mechanism of the peak [7–12]. In Ti–Nb alloy, it is extremely difficult to remove oxygen even though the heat treatment is conducted at high vacuum. Therefore, the specimens contain oxygen under the condition of non-vacuum heat treatment. The present oxygen concentration is estimated to be about 0.05 (wt.%) in the present Ti-35.4Nb alloys from the peak height according to Ref. [7] although O is not designedly introduced into the sintered Ti–Nb alloys in all processing steps. If the oxygen atoms are located in the octahedral positions of the alloys with bcc structure, they will produce relaxation process under the application of cycle stress

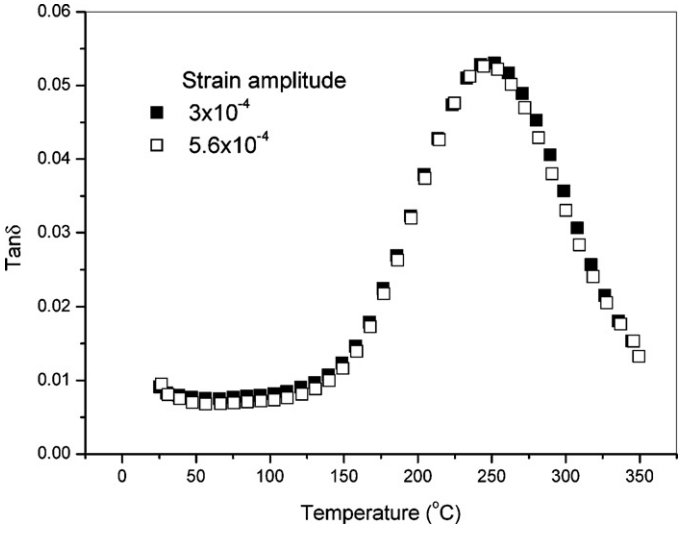

Fig. 2. Tanδ as a function of temperature for the water-quenched Ti-35.4 Nb alloy for different amplitude ($f = 1$ Hz).

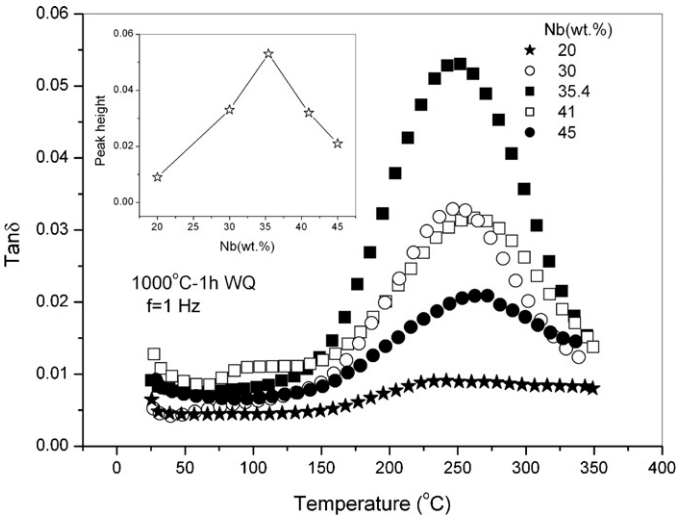

Fig. 3. The dependence of the peak height on Nb content for the water-quenched Ti–Nb alloys ($\varepsilon = (2.4\text{-}4.3) \times 10^{-4}$, $f = 1$ Hz).

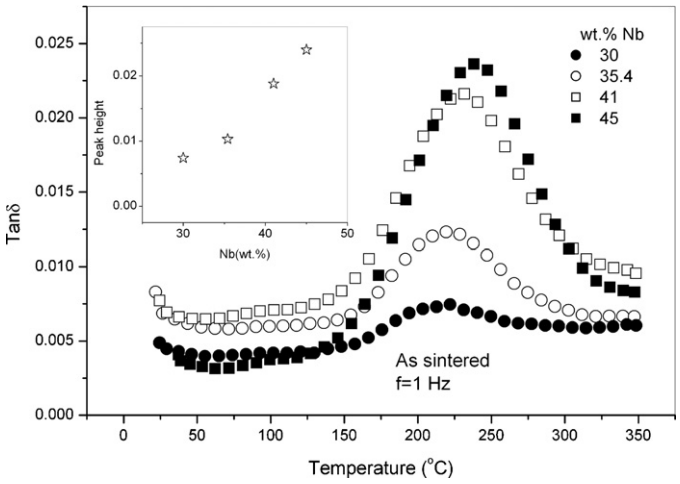

Fig. 5. The dependence of the peak height on Nb content for the as-sintered Ti–Nb alloys ($\varepsilon = (2.5\text{–}4) \times 10^{-4}$, $f = 1$ Hz).

and an internal friction peak known as the Snoek peak will appear on the internal friction-temperature curve. The present activation energy of the relaxation peak is also close to the activation energies for intrinsic diffusion of Ti and Nb in the Ti–Nb alloys, which are 164.22 kJ/mol (1.7 eV) for Ti and 177.66 kJ/mol (1.84 eV) for Nb, respectively, according to Ref. [14]. Thus, the present relaxation process may be related to not only oxygen but also the metallic atoms such as Ti and Nb. The interaction of Nb–O may be involved in the internal friction peak according to Ref. [13]. From Fig. 3, it can be seen that the peak height depends on Nb content and varies non-monotonously with Nb content for the quenched alloys. The peak height presents a maximum in the vicinity of 35 wt.% Nb, resulting from the variation of the stability and amount of β_M with Nb content.

Fig. 4 presents the internal friction-temperature curves of as-sintered Ti-35.4Nb alloy. It can be seen that the internal friction peak still exists although the peak height is much smaller compared with the water-quenched Ti-35.4Nb alloy, indicating that the producing procedure has an effect on the internal friction peak. The peak in the as-sintered specimen has also relaxational feature from its peak temperature dependence on frequency. The activation energy can be calculated to be $H_s = 2.13 \pm 0.2$ eV and $\tau_{0s} = 2.7 \times 10^{-23\pm2}$ s, respectively. In contrast, for as-sintered Ti–Nb alloys, the variation of the peak height with Nb content is different from that of the water-quenched alloys, as shown in Fig. 5. Obviously, the peak height increases monotonously with increasing Nb content in the as-sintered alloys.

3.2. The relationship of the internal friction peak with microstructures

β-type Ti–Nb alloys exhibit single disordered bcc β phase at higher temperatures. If A specimen at higher temperatures with β phase is water-quenched, the high temperature β phase will be retained to room temperature, forming a so-called metastable β phase (β_M), which is then partly or completely transformed into

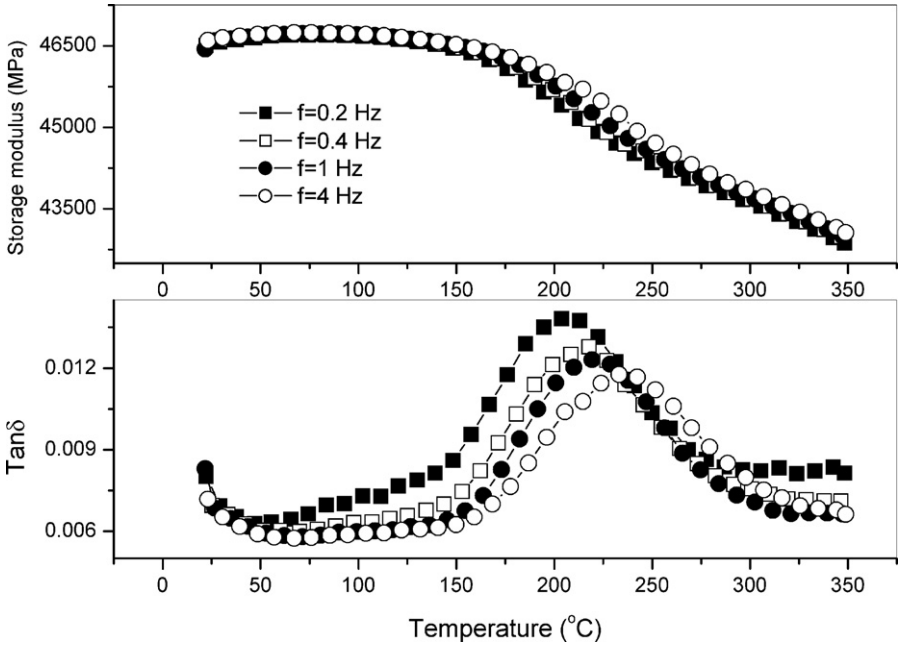

Fig. 4. Tanδ and storage modulus as a function of temperature for the as-sintered Ti-35.4 Nb alloy at different vibration frequencies ($\varepsilon = 3.7 \times 10^{-4}$).

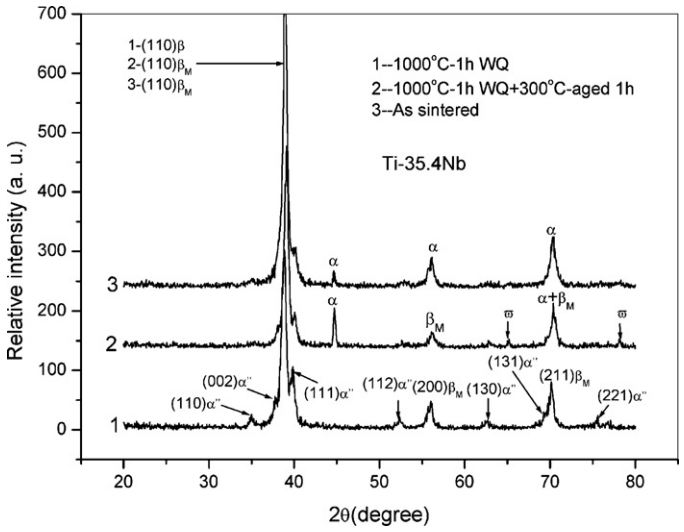

Fig. 6. XRD results of three Ti-35.4Nb specimens with different heat treatments.

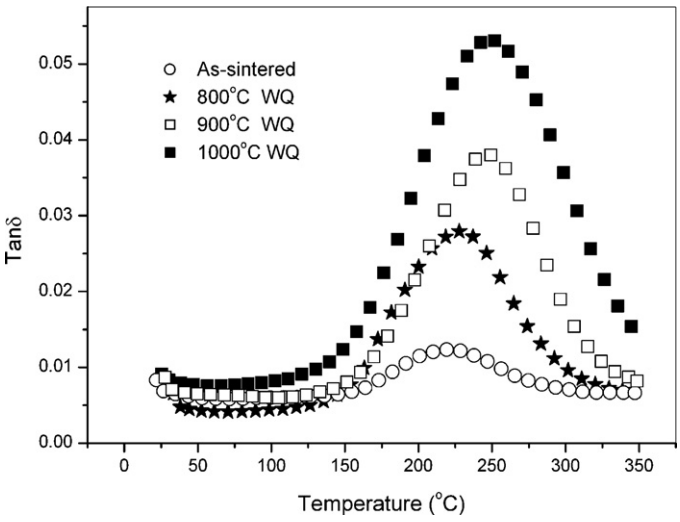

Fig. 7. Influence of water-quenching temperature on the relaxation strength for Ti-35.4Nb specimen with different quenching temperature ($\varepsilon = (2.8–3.7) \times 10^{-4}$, $f = 1$ Hz).

either hexagonal martensite (α′) or orthorhombic martensite (α″) in the Ti–Nb alloys with lower Nb content [15]. When Nb concentration exceeds about 25 wt.%, the final microstructures will contain the retained β_M, i.e., β_M can not completely be transformed into α″. When Nb content is over 38 wt. %, β_M is completely kept to room temperature. Therefore, the final microstructures consist of α″ and β_M for the water-quenched alloys with 25-38 wt.% Nb [16]. Furnace-cooled alloys always form α and β (β_S) phases according to Ti–Nb binary phase diagram [1]. According to Ref. [16], the present water-quenched Ti-35.4Nb alloy should possess α″ and β_M, which is also confirmed by the XRD results in Fig. 6. Obviously, the quenched Ti-35.4Nb alloy contains α″ and β_M phases and the as-sintered specimen exhibits both α and β_S phases. From Fig. 3, no obvious internal friction peak can be resolved for the quenched Ti-20Nb alloy. This indicates that the peak does not appear in the specimen without β phase since this Ti-20Nb quenched alloy contain only α′ and α″ according to Ti–Nb binary phase diagram [1]. Therefore, the internal friction peak of the quenched alloys is closely linked to β_M.

It has been experimentally confirmed that as-sintered specimens possess α and β_S phases. According to Ti–Nb binary phase diagram [1], the amount of stable α phase decreases and that of β_S phase increases with increasing Nb concentration. From Fig. 5, it can be deduced that the peak height increases with increasing the amount of the β_S phase, indicating that the internal friction peak in as-sintered alloys is also correlated to the β phase.

The β_M with bcc structure has many octahedral positions. The positions are octahedral of the types (1/2, 0, 0) and (1/2, 1/2, 0). The ensuing strain tensor has local tetragonal symmetry with one of the principal axes coinciding with one of the three main directions ⟨1 0 0⟩ of the bcc matrix [3]. The anelasticity can be caused by stress-induced migration of interstitial atoms in the octahedral positions of bcc lattices. Nevertheless, in Ti–Nb alloys, oxygen atoms were claimed to be trapped by the substitutional atoms, therefore the Snoek-type relaxation can be corresponded to O atomic jumps in bcc β phase or their interactions between metallic atoms and interstitial atoms [8]. These interactions may include Nb–O, Nb–N, Ti–O, Ti–O–O and Nb–O–O in β phase [9,10].

3.3. The mechanisms of effects of Nb concentration and heat treatment on the relaxation

It is known that the stable α is a rich-Ti phase and the β_S is a rich-Nb phase. The amount of the β_S increases when Nb content is increased for the as-sintered Ti–Nb alloys since Nb is a β phase stabilizer. This indicates that the number of Nb–O atomic pairs in as-sintered Ti–Nb alloys may increase when Nb content is increased or that the interaction in Nb–O atomic pairs is strengthened, resulting in the increase of the peak height with increasing Nb content with increasing Nb content.

It has been known that the β_M can be obtained by quenching and the β_S is formed by annealing [3]. The present as-sintered alloys are similar to the annealed alloys in their structures. For the Ti-35.4Nb alloy, it can be seen that the peak height in the quenched specimen is much higher than that in the as-sintered specimen by comparing Fig. 1 with Fig. 4, indicating that the peak height has also dependence on the stability of the β phase. On one hand, the amount of the β_M phase increases with the increase of Nb content. On another hand, the stability of β phase increases with increasing Nb content even though for the quenched Ti–Nb alloys since Nb element is β stabilizer [17], which suppresses the further increase of the β_M phase in amount and even promote the formation of β_S when Nb content is further raised. If so, the peak height and β_M amount have similar dependency on Nb content in the quenched alloys. The peak height will not be influenced by heat treatment when Nb content is over certain value, in accordance with the present results. Fig. 7 shows the influence of the water-quenching temperature on the relaxation strength. It can be seen that the peak-height increases with increasing the quenching temperature. When the quenching temperature is raised, O atoms dissolved in solution are increased, resulting in the increase of the peak height. It can be deduced that oxygen jumps are main contributions to the internal friction peak for the water-quenched alloys in addition to the *s–i* (e.g., Nb–O) interactions.

Fig. 8 shows the dependence of the peak on the thermal cycling times for the quenched Ti-35.4Nb alloy. It can be seen that the peak height is gradually decreased and storage modulus is elevated when the thermal cycling times are increased. It is known that the quenched Ti-35.4Nb alloy possesses β_M. The β_M can firstly be transformed into a transition ω phase when it is aged at intermediate temperature and eventually the stable α and β_S phases are formed [18,19], which is confirmed by XRD results. From Fig. 6, it can be seen that the specimen of the Ti-35.4 Nb aged at 300 °C for 1 h contains the ω phase. Therefore, β_M amount is decreased with the increases of thermal cycles, causing the peak height to decrease. In addition, the increase in the storage modulus is attributed to the increase of the volume fraction of ω [19] since ω phase is larger

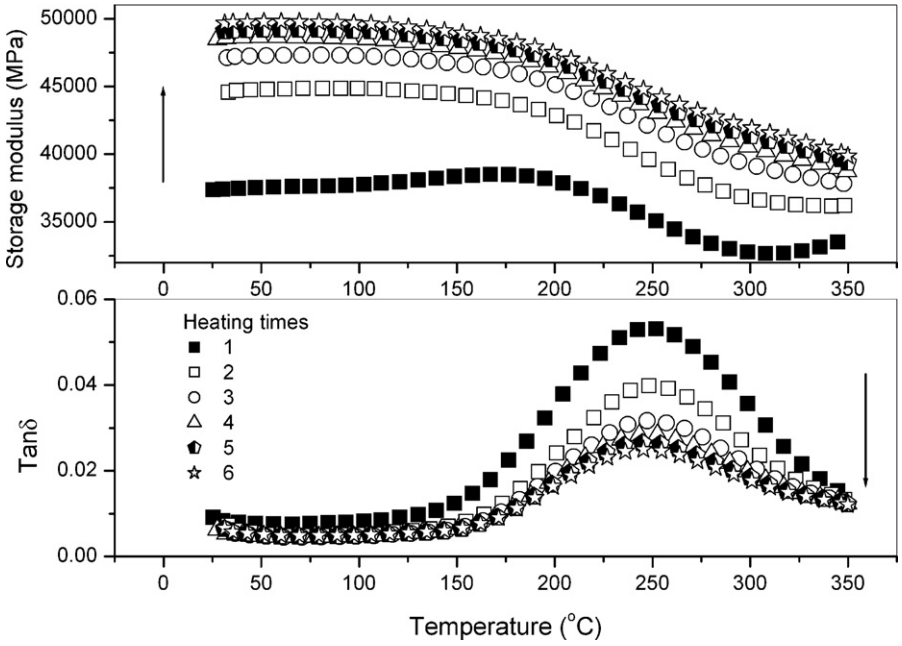

Fig. 8. Influences of thermal cycles between room temperature and 350 °C on Tanδ and storage modulus for the water-quenched Ti-35.4 Nb alloy ($\varepsilon = 3 \times 10^{-4}$, $f = 1$ Hz).

than β phase in modulus and hardness [20]. Generally, the aging can decrease the amount of O atoms in solution, which can also cause the peak height to reduce.

A diffusional-displacive transformation is characterized by a strong interaction of its displacive component with stress when temperature is high enough to allow diffusion to occur. Such a stress-induced transformation is time-dependent and strongly dependent on temperature [21]. This indicated that the volume fraction of formed ω depends on the aging time and increases with the increase of aging time [22,23]. Therefore, the volume fraction of ω phase should increase with increasing the thermal cycles when the internal friction of the water-quenched Ti-35.4Nb alloy is circularly measured in the temperature range from room temperature to 350 °C. The increase in the volume fraction of ω will cause the storage modulus of the specimen to increase.

It should be pointed out that the storage modulus in the water-quenched Ti-35.4% Nb specimen is smaller than that in the as-sintered Ti-35.4% Nb alloy, which results from the difference in microstructures of two specimens. As-sintered Ti-35.4% Nb alloy has stable α and β_S phases, while the water-quenched Ti-35.4% Nb specimen possesses β_M and α″. β_M and α″ have lower storage modulus [20]. However, the detail mechanism of the modulus difference should be further investigated for the two specimens.

4. Conclusion

There is a relaxational internal friction peak in sintered Ti–Nb alloys. The peak height depends on Nb content and heat treatment. No internal friction peak can be found in the Ti–Nb alloys with low Nb content. The peak is related to β_M phase in the water-quenched alloys and to β_S phase in the as-sintered alloys. Oxygen jumps in lattice and the interactions between O and Nb are contributed to the internal friction peak in β_M for the water-quenched alloys and in β_S phase for the as-sintered alloys.

Acknowledgements

This work is supported by Jiangsu Government Scholarship for Overseas Studies in China.

References

[1] J.L. Murray, Phase Diagram of Binary Titanium Alloys, Materials Park, ASM, Ohio 1987.
[2] M.S. Blanter, I.S. Golovin, H. Neuhäuser, H.-R. Sinning, Internal friction in metallic materials, in: A Handbook (springer series in materials science), vol. 90, Springer, Berlin Heidelberg, Berlin, Germany, 2007.
[3] A.S. Nowick, B.S. Berry, Anelastic Relaxation in Crystalline Solids, Academic Press, Now York and London, 1972.
[4] H. Saitoh, N. Yoshinaga, K. Ushioda, Acta Mater. 52 (2004) 1255.
[5] I.S. Golovin, S.B. Golovina, Phys. Metals Metallogr. 102 (2006) 593–603.
[6] I.S. Golovin, S.B. Golovina, O.A. Sokolova, Phys. Metals Metallogr. 105 (2008) 193–201.
[7] F. Yin, S. Iwasaki, D. Ping, K. Nagai, Adv. Mater. 18 (2006) 1541.
[8] F. Yin, L. Yu, D. Ping, S. Iwasaki, Mater. Sci. Forum 614 (2009) 175.
[9] O. Florêncio, F.W.J. Beta, C.R. Grandini, H. Tejima, J.A.R. Jodão, J. Alloys Comp. 211–212 (1994) 37.
[10] L.H. Almeida, C.R. Grandini, R. Caram, Mater. Sci. Eng. A 521–522 (2009) 59.
[11] F. Yin, L. Yu, D. Ping, Mater. Sci. Eng. A 521–522 (2009) 372.
[12] T.C. Niemeyer, J.M.A. Gimenez, L.H. Almeida, C.R. Grandini, O. Florêncio, Met. Res. 15 (2002) 143.
[13] L. Yu, F. Yin, D. Ping, Phys. Rev. B 75 (2007) 174105.
[14] C.S. Hartley, J.E. Steedly, L.D. Parsons, in: J.A. Wheeler, F.R. Winslow (Eds.), Diffusion in Body-centered Cubic Metals, American Society for Metals, Ohio, 1965.
[15] S. Miyazaki, H.Y. Kim, H. Hosoda, Mater. Sci. Eng. A 438–440 (2006) 18.
[16] L.A. Matlakhova, A.N. Matlakhov, S.N. Monteiro, Mater. Charact. 59 (2008) 1234.
[17] M. Abdel-Hady, K. Hinoshita, M. Morinaga, Scripta Mater. 55 (2006) 477.
[18] H.J. Rack, D. Kalish, K.D. Fike, Mater. Sci. Eng. 6 (1970) 181.
[19] Y. Mantani, M. Tajima, Mater. Sci. Eng. A 442 (2006) 409.
[20] Z. Fan, Scripta Metall. Mater. 29 (1993) 1427.
[21] X. Ren, M. Hagiwara, Acta Met. 49 (2001) 3971.
[22] D.H. Ping, Y. Mitarai, F.X. Yin, Scripta Mater. 52 (2005) 1287.
[23] H.Y. Kim, J.I. Kim, T. Inamura, H. Hosoda, S. Miyazaki, Mater. Sci. Eng. A 438–440 (2006) 839.